Journal of Electronics and Electrical Engineering
https://ojs.wiserpub.com/index.php/JEEE

Research Article

Floating Photovoltaic Solar in Australia-A Feasibility Study

Sara Deilami*, Hassan Ali Ozgoli, Leonardo Callegaro, Foad Taghizadeh, Kyoung Hoon Kim

School of Engineering, Macquarie University, Sydney, Australia
E-mail: sara.deilami@mq.edu.au

Received: 16 September 2024; **Revised:** 21 November 2024; **Accepted:** 22 November 2024

Abstract: The global adoption of solar power is accelerating, with Australia leading in per capita solar power generation. However, ground photovoltaic (GPV) systems face limitations due to low surface power density and land use constraints. Floating photovoltaic (FPV) systems provide a viable alternative by utilizing waterbodies, such as hydropower reservoirs, to increase efficiency through evaporative cooling and address land-use constraints. This paper investigates the technical and economic feasibility of integrating FPV with hydropower plants (HPPs) in Australia, specifically focusing on Burrendong Dam in New South Wales. Through the analysis of global FPV efficiency studies and theoretical energy modeling, using Trina Solar's 210 Vertex modules, the study demonstrates that FPV systems outperform GPV systems by approximately 2.54% in average efficiency and achieve a 5.51 °C lower panel temperature. Although FPV systems entail 20% higher initial costs, their efficiency and land-use benefits support their viability. This research fills a critical gap in localized FPV studies, offering an in-depth evaluation of environmental, financial, and technical aspects and providing essential insights for FPV development in Australia's renewable energy sector.

***Keywords*:** Floating Photovoltaic Systems (FPV), renewable energy integration, hybrid FPV, hydropower, solar power efficiency, environmental impacts

1. Introduction

As of 2023, solar power provides around 4.5% of the world's electricity. This reflects the rapid growth in solar capacity investments and installations globally. The increase is driven by significant policy support, technological advancements, and decreasing costs of solar PV systems [1]. The cost of large-scale solar electricity declined by 85% between 2010 and 2020. The International Renewable Energy Agency (IRENA) reports that the levelized cost of electricity (LCOE) for large-scale PV facilities fell by 3% year on year to $0.049 kWh in 2022 [2]. In 2023, renewable energy sources contributed approximately 40% of Australia's total electricity generation. This is a significant increase from previous years and aligns with Australia's goal of achieving 82% renewable energy by 2030. Solar energy alone accounted for around 16% of the total electricity generation, with rooftop solar contributing 11.7% and large-scale solar 6.6% [3]. Australia also leads globally in solar power generation per capita, reaching 1331 W/capita by the end of 2023 [4]. To further enhance this positive trajectory, the New South Wales (NSW) Government has introduced Renewable Energy Zones, aimed at expanding renewable energy generation and phasing out coal power stations [5]. These initiatives align with the United Nations' Sustainable Development Goals, which seek to establish a sustainable and prosperous future for all nations [6].

DOI: https://doi.org/10.37256/jeee.3220245731

One of the most glaring weaknesses of ground photovoltaic systems (GPV), and other renewable energy sources, is its low surface power density, which is a measurement for power generated per given area [7]. Compared to natural gas, solar power has a surface power density that is about 73 times lower. One way to mitigate this is with floating photovoltaic systems (FPV), which can be installed on waterbodies with little alternative use such as an artificial waterbody of a hydropower (HPP) station.

Extensive research on the feasibility of hybrid FPV/HPP stations has been conducted in various regions; however, a significant gap remains in understanding how these systems perform in Australia's unique environmental and regulatory context. This study addresses this gap by exploring the integration of FPV systems with hydropower plants, focusing on Burrendong Dam in New South Wales. Unlike prior studies, which have been predominantly global in scope, our research offers localized insights into the environmental, technical, and financial viability of FPV systems in Australia. This approach not only contributes to the growing body of knowledge on renewable energy systems but also aligns with Australia's national goals for increasing renewable energy capacity and addressing land-use constraints.

The environmental effects of solar power are minimal. During operation, PV modules do not produce any harmful emissions. However, the manufacturing process results in some greenhouse gas emissions. The life-cycle greenhouse gas emissions of various energy sources in $gCO_2eq\ kWh^{-1}$ (median life-cycle CO_2 equivalent) are compared in Figure 1 [8]. These measurements cover the total potential for CO_2 emissions of energy sources, from material mining, construction, and operation to decommissioning.

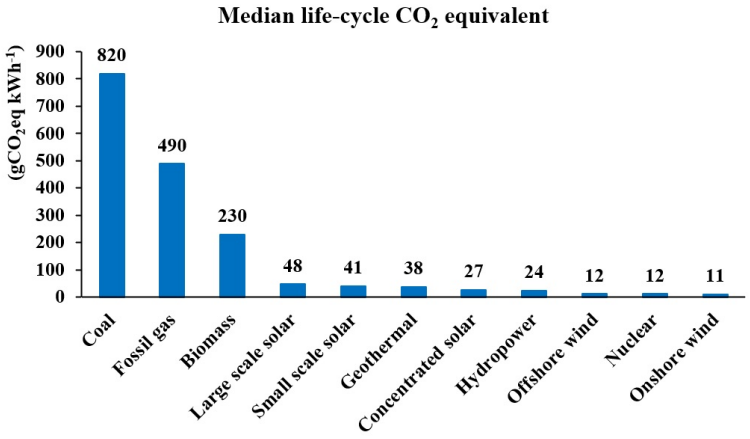

Figure 1. Life-cycle greenhouse gas emissions of various energy sources in $gCO_2eq\ kWh^{-1}$ [8]

Another factor by which solar power can be compared to other energy sources is the surface power density. This measurement calculates the electricity generated per surface area of Earth by each energy source throughout its life cycle, including material acquisition, operation, and decommissioning [7]. Most non-renewable energy sources have considerably higher power density compared to renewable energy sources, and this is one of the most significant limiting factors of renewable energy [9]. Figure 2 presents the energy sources and their median power density.

Kamuyu et al. (2018) develop predictive models for FPV module temperatures, incorporating ambient temperature, solar irradiance, wind speed, and water temperature [10]. The study highlights FPV systems' enhanced performance, achieving up to 16% higher energy efficiency than rooftop PVs, attributed to reduced operational temperatures. Notably, 89% of FPV energy production occurs when module temperatures are below 40 °C, compared to 68% for land-based systems. With predictive errors of 2–4%, these models offer reliable tools for optimising FPV design and energy output under varying conditions.

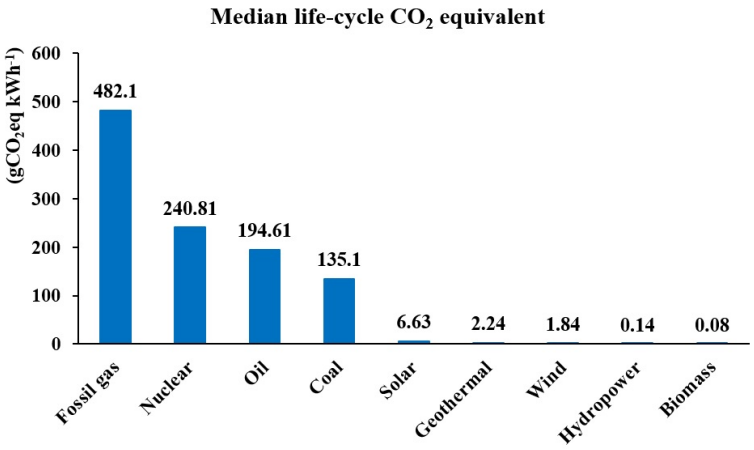

Figure 2. Energy sources and their median power density [8]

The efficiency difference in Table 1 represents the percentage by which the FPV system's energy output exceeds or falls short of that of a comparable GPV system under similar conditions. These differences can be attributed to various factors, such as enhanced cooling effects from the waterbody, which can improve the performance of solar panels.

Table 1. Past studies on the comparison of efficiency of FPV and GPV

Reference	Efficiency difference (%)	Type of solar PV	Remarks
Kamuyu CLW, et al. 2018 [10]	16	Monocrystalline	Analysis of FPV in US dams
Kim, Sukarso. 2020 [11]	2	Thin film	Efficiency improvements in FPV-China
Spencer, RS, et al. 2019 [12]	10.5	Polycrystalline	Vaigai dam 22 MW case study
Liu LL, et al. 2017 [13]	13.5	Monocrystalline	FPV vs. land PV comparison
Salman M. 2024 [14]	10	Thin film	Large-scale FPV, Skadar Lake
Yadav N, et al. 2016 [15]	11	Various (mono, poly)	FPV projects review 2007–2013
Djurisic, Durković. 2015 [16]	15.5	Polycrystalline	80 W FPV study in Malaysia
Trapani, Redón. 2017 [17]	14	FRP-integrated Polycrystalline	FRP-based FPV system
Majid ZAA, et al. 2014 [18]	14.5	Polycrystalline	Malaysia FPV performance
Lee YG, et al. 2014 [19]	13	Monocrystalline	K-water FPV case studies
Azmi MSM, et al. 2013 [20]	12	Thin film	Comparison of FPV and land PV
Choi YK. 2014 [21]	11	Polycrystalline	FPV environmental impacts

Manoj Kumar et al. [22] have shown the potential of FPV systems in improving solar energy output. It was found that FPV systems can produce up to 10.2% more power than ground-mounted systems due to reduced thermal losses and enhanced cooling from water. Also, they demonstrated that integrating FPV with hydropower infrastructure can significantly boost power generation and minimize energy imbalances, making FPV a promising renewable energy solution for regions like Australia.

Floating solar photovoltaic systems offer higher energy yields (0.6% to 4.4% more) and efficiency gains (0.1% to 4.45% improvement) compared to land-based installations. Despite scattered research, consolidating insights reveal advancements in structure design, monitoring capabilities, and potential technologies like tracking systems and bi-facial panels. Integration in marine environments and reservoirs shows promise, but addressing safety, policy, and environmental challenges is critical for sustainable energy adoption [23].

Four models were proposed in a study by Atiqur Rahaman et al. [24] to predict module temperatures of FPV systems, emphasizing the inclusion of water temperature as a critical parameter. The study demonstrated up to a 3% higher efficiency compared to traditional ground-based models, underscoring the efficacy of water cooling in enhancing FPV system performance. The FPV system achieved an electrical efficiency of 17.05%, outperforming both the Sandia model (17.01%) and the Kamuyu FPV model (17.10%).

One of the biggest challenges of a large photovoltaic system is its land use, especially in Australia, where it averages about 50–70 MWp km^{-2} [25]. In contrast, as of 2017, more than 400,000 km^2 of man-made reservoirs exist globally, providing substantial opportunities for hybridisation with FPV systems [26]. These reservoirs, primarily underutilised for energy production, offer a unique advantage in mitigating land use challenges associated with large-scale photovoltaic systems.

The reservoir provides shade-free areas with high sunlight reflection for FPV panels, which is advantageous because the increased reflection can enhance the amount of solar radiation received by the panels. This can lead to improved efficiency and higher energy output of the FPV system. FPV panels also benefit from evaporative cooling effects, making them about 15% more effective than their land-installed counterparts [27]. The reservoir also benefits from FPV. A study revealed that covering 30% of its surface area can reduce evaporative water loss by up to 49% [28]. A waterbody with less than 60% shading has been shown to improve the ecological condition while avoiding harm to the native ecosystem [29].

HPP can complement FPV by acting similarly to a battery [30]. Since FPV has an irregular power output that depends on weather conditions, HPP can be used during hours of low solar irradiation or during hours of surplus generation to pump water to an upper reservoir using power generated by FPV.

Introducing FPV to an existing HPP with ample transmission line capacity may also increase the utilization rate of the existing infrastructure [31]. HPPs are often located far from load centers and have dedicated transmission lines. These specific transmission lines are often underutilized, with only a fraction of their total capacity being used, which increases the cost of energy due to high infrastructure costs. By installing FPV to take advantage of this circumstance, FPV can make use of the existing underutilized infrastructure, decreasing the overall cost of energy more than having two separate systems.

One instance where this relationship can be utilized is when a lower reservoir of an HPP is over capacity and the transmission line is left unused. Specifically, Burrendong Dam's water level, as of October 2022, has been over 100% since September 2021 [32]. Burrendong Dam cannot release enough water to keep its level under capacity without causing floods downstream. This presents a significant issue, as managing the water level is crucial to prevent flooding and ensure dam safety. FPV could help mitigate this problem by utilizing the reservoir surface for energy production, thereby reducing evaporation and lowering the water level indirectly. Additionally, the power generated by FPV can be used to pump water to upper reservoirs or for other purposes, further aiding in water level management.

However, FPV demands higher initial costs than its land-based counterparts [33], and its materials must be carefully selected and monitored to prevent water quality degradation. Assuming FPV cells have 0% UV light transparency, worst-case water quality analysis indicates that up to 10% of a reservoir's surface area can be covered without disrupting the microbial balance of the water [34]. The leaking of heavy metals, most notably lead and cadmium, was measured in a study to be neither an imminent nor a future environmental risk [35]. However, the authors noted the possibility that defective or damaged units allowing water inside the panel could leak heavy metals.

Compared to GPV, FPV is reported to have a LCOE that is 20% higher. This difference is due to FPV's floats and anchoring system, resulting in a far higher structural cost. The water body also introduces more installation, operation, and maintenance hazards. Along with the risk factors associated with GPV, such as heat stress and repetitive strain injury, the water body presents dangers of increased risk of electrical leakage and heat stress [36].

All facets of GPV systems are extensively researched globally and within Australia. However, FPV systems are relatively new, and there is a significant lack of research on their viability in Australia. This gap in local research likely contributes to the limited number of FPV projects in the country. Aggregating scattered global data about FPV and applying it to Australia's unique climate to study the financial and technical feasibility would be a valuable contribution. This research aims to bridge the knowledge gap, offering insights that could spark further interest and development of FPV technology in Australia.

2. Floating photovoltaic system

FPV utilizes the same photovoltaic effect and the same modules as GPV. While care must be taken to ensure an appropriate Ingress protection (IP) rating for the electronics, as FPVs are more exposed to liquids, the main difference is structural.

2.1 *Floating photovoltaic system structure*

Pontoon: Pontoons or floats are devices with enough buoyancy to support themselves and any other load on top of them. Pontoons are often modular in design, allowing flexibility in a PV system design. Singapore's floating solar farm in Tengeh, for example, used UV-resistant, food-grade high-density polyethylene to minimize the impact on the environment [37].

PV Modules: While most standard crystalline photovoltaic modules can be used for an FPV project, special care must be taken to select modules with an IP rating of at least 66, which provides total protection against dust and protection against strong jets of water. Damaged PV modules have the possibility of leaking heavy metals into the environment [35].

Mooring: A mooring is a permanent structure that holds pontoons in place and is installed underwater. The installation of the mooring can be dangerous and expensive, depending on factors such as water depth, water current, and the floor of the waterbody.

Cables: Cables and connectors can either run above or under water. In both cases, cables and connections must have appropriate IP ratings against water, heat, and dust.

Figure 3 shown below lists realised and estimated FPV investment costs around the world from 2014 to 2018. The investment costs for FPV systems in India during 2018, as depicted in Figure 3, show consistent values primarily due to the nature of the auction-based pricing approach. These auctions ensure cost standardisation by setting competitive price ceilings for projects, leading to uniform costs across regions. Furthermore, the values in the figure are compiled from various media releases and industry reports, reflecting an aggregation of publicly available data rather than individual project-specific details. This approach aligns with the source description of the figure.

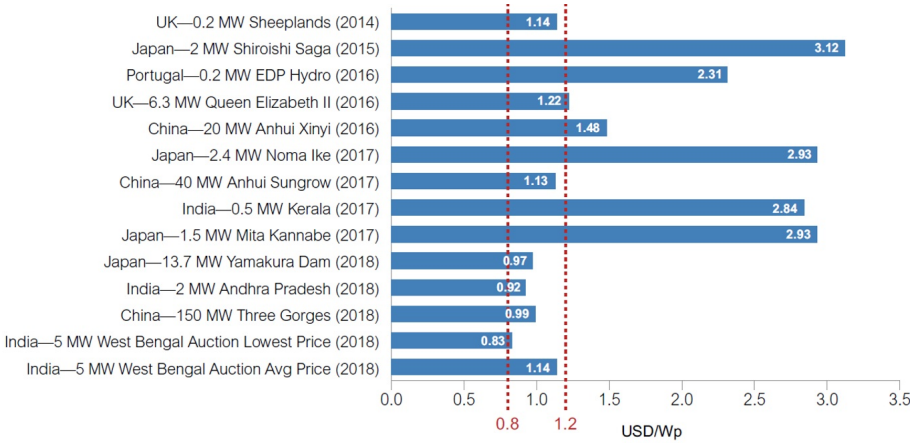

Figure 3. Investment costs of floating PV in 2014–2018 (realized and auction results) [38]

Japan has relatively high investment costs due to elevated labour expenses, stricter land-use regulations, and the financial structure supported by feed-in tariffs (FiTs). The high FiTs in Japan are designed to encourage renewable energy deployment but indirectly increase overall costs by creating a premium market environment. On the other hand, India and China benefit from significantly lower costs due to a combination of lower labour rates, supportive policies, and large-scale local manufacturing capabilities. The FiTs in these countries are structured to prioritise cost-efficiency, contributing to the reduced investment requirements for solar energy projects [38].

FPV systems offer several advantages that can offset their higher initial investment costs over time. As it has been indicated by Semeskandeh et al. [39], FPV systems benefit from enhanced energy production efficiency due to the cooling effects of water, which reduce panel temperatures by an average of 11 °C, and can achieve up to 19.47% more energy output compared to GPV systems. Additionally, FPV installations minimise land use requirements and can reduce water evaporation rates by as much as 70%, further contributing to their environmental and economic value.

2.2 *Hybrid floating PV/hydropower system*

The integration of FPV systems with HPPs presents a technically advanced solution aimed at optimizing the efficiency of both renewable energy sources. Unlike ground-mounted photovoltaic systems, FPV arrays benefit from the cooling effect of the water surface, which helps to lower the operating temperature of the solar panels, thereby improving their overall performance and increasing energy output by up to 2.54% [25]. This enhanced efficiency is particularly important in maximizing the use of existing water bodies, especially where land availability is constrained.

At Burrendong Dam, the installation of FPV arrays on the reservoir demonstrates the potential of hybrid FPV-HPP systems to not only augment energy generation but also contribute to water conservation. By reducing evaporative water loss this hybrid system addresses one of the critical environmental concerns in regions prone to drought [26]. The FPV system's capacity to operate alongside hydropower further ensures the efficient use of reservoir surfaces, leading to an estimated 10% increase in annual energy production [27].

From an economic perspective, the integration of FPV with HPPs offers a cost-effective solution by utilizing existing transmission infrastructure, reducing the need for additional investments in land or electrical grid extensions [28]. This synergy between the two systems enables a more balanced energy supply, particularly during periods of high solar output, when the hydropower plant can act as a stabilizing energy source by storing excess energy generated by the FPV system [29].

In addition to maximizing energy generation, the underutilized transmission lines of many HPPs can be leveraged by FPV systems, further decreasing the LCOE for both systems. HPPs often have surplus transmission capacity, especially during periods of low water flow, when hydropower generation is limited. By installing FPV systems to utilize this spare capacity, overall infrastructure utilization rates increase, thereby lowering energy costs. In the case of Burrendong Dam, this approach can be particularly beneficial when water levels are high, as was the case from September 2021 to October 2022, when water levels exceeded 100% of the dam's capacity [31].

The operational challenges posed by high water levels at Burrendong Dam, particularly the need to manage controlled water release to prevent downstream flooding, further underscore the importance of balancing hydropower and FPV generation [32]. The hybrid system at Burrendong Dam provides a practical solution by generating additional energy during periods when hydropower production is constrained by the need to regulate water discharge. This ensures a continuous energy supply while addressing flood risk management, particularly in downstream areas reliant on controlled water release [40].

3. Methodology

3.1 *Best candidate/selection sites*

The surface area of a Hydropower Plant (HPP) reservoir is a key factor determining the maximum number of Floating Photovoltaic (FPV) panels it can support. Additionally, the proximity of a potential FPV site to the power station is crucial for minimizing costs. The total cost of flotation devices depends on factors such as the average water level, water level variation, and the composition of the waterbody floor. The site selection process also incorporates the NSW government's Renewable Energy Zones plan. Figure 4, derived from a National Renewable Energy Laboratory report, examines variables influencing the LCOE of FPV systems. Unlike GPV, FPV systems incur significant floatation costs related to the floating infrastructure. Environmental factors such as wind load, snow load, water depth, and water level variation also influence the LCOE of FPV systems.

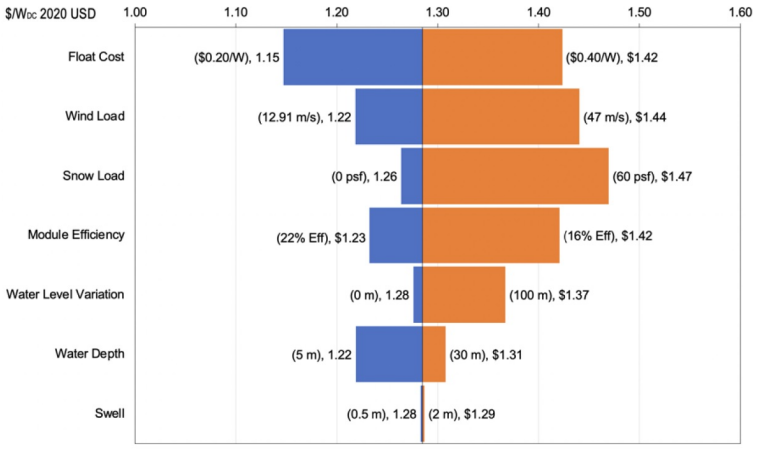

Figure 4. Sensitivity analysis of FPV systems [41]

Another critical factor in site selection is the capacity of existing transmission infrastructure and its ability to handle additional capacity. The generator specifications and performance metrics have been obtained for application in this study. The total annual inverter output of an FPV system will be limited to 50% of a hydropower station's total annual output to maintain grid stability and reliability. Among the candidates listed in Table 2, Burrendong Dam has been selected due to its ease of access for construction and maintenance, its location within NSW's Central West Renewable Energy Zone, proximity to the power station, absence of dense woodland near the site, relative proximity to a major load center, and the lack of registered Aboriginal sites in the area. Figures 5 and 6 further illustrate the suitability of this site.

Table 2. List of potential sites and their key parameters [42]

Power station	Max capacity (MW)	Reservoir area (km^2)	Pumped storage	Distance from nearby city
Tumut 3, New South Wales (NSW)	1500	921	Y	3 h from Canberra
Wivenhoe, Queensland (QLD)	500	203	Y	1 h from Brisbane
Gordon, Tasmania (TAS)	432	278	N	2.5 h from Hobart
Poatina, Tasmania (TAS)	300	176	N	1 h from Launceston
Reece, Tasmania (TAS)	231	2.22	N	2.5 h from Devonport
Kangaroo Valley, New South Wales (NSW)	160	5.4	Y	2.5 h from Sydney
Bendeela, New South Wales (NSW)	80	0.2	Y	2.5 h from Sydney
McKay Creek, Victoria (VIC)	150	2.2	N	5 h from Melbourne
Dartmouth, Victoria (VIC)	150	63	N	5 h from Melbourne
John Butters, Tasmania (TAS)	144	54	N	4 h from Hobart
Tungatinah, Tasmania (TAS)	125	0.4	N	2 h from
Eildon, Victoria (VIC)	120	138	N	2 h from Melbourne
Burrendong, New South Wales (NSW)	19	89	N	1 h from Orange & Dubbo

Figure 5. Photo of Burrendong dam [40]

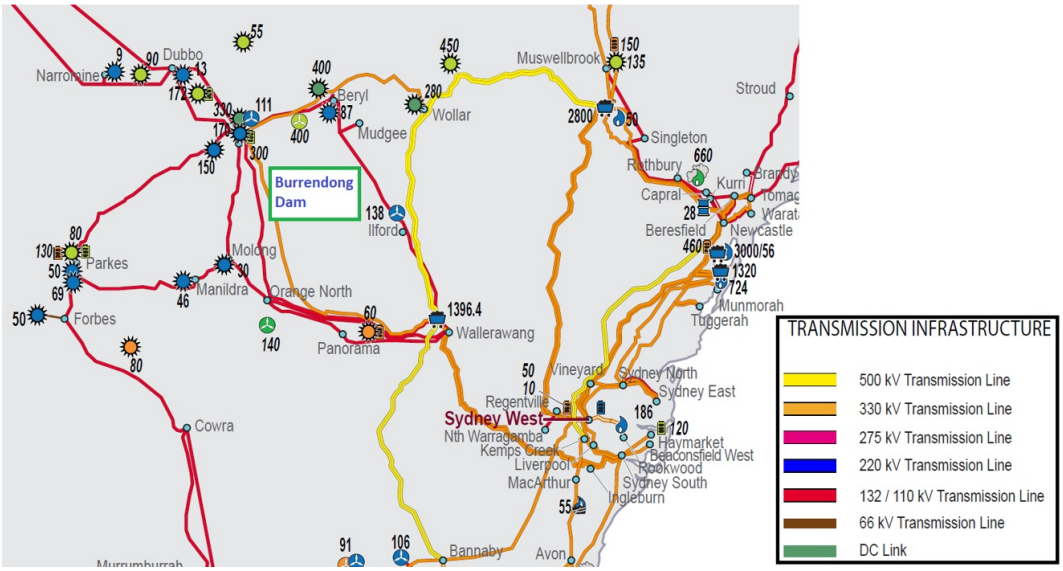

Figure 6. Map of high voltage electricity transmission network in NSW

Dense woodland near the site can pose challenges for the construction and operation of a solar project like FPV. It may require clearing of vegetation, potentially disrupting local ecosystems and habitats [43]. Additionally, dense woodland can affect solar irradiance and create shading issues, impacting the efficiency and performance of solar panels.

4. System modeling

4.1 *Theoretical calculations*

4.1.1 *PV module*

For the analysis, Trina Solar's 210 Vertex modules were selected. These modules have a power rating of 210 watts and utilize multicrystalline technology. The total number of PV modules needed for the simulation (NPV) will be calculated based on the required power output (P) and the maximum capacity of each module (R).

$$N_{PV} = \frac{P}{R} \tag{1}$$

R can be expressed as:

$$R = \varphi_0 t_s \tag{2}$$

where φ_0 is the rated capacity of an individual PV module, and t_s is the number of hours with maximum solar irradiance in a day.

In the design of the FPV system at Burrendong Dam, the photovoltaic panels are mounted at a fixed tilt angle of 15°. This angle was selected based on the geographic location and irradiance profile of the site. Additionally, this tilt provides an optimal balance between maximizing energy production and ensuring the structural stability of the floating platform, which is crucial given the wind and water conditions in the area. The selected angle also helps mitigate issues such as wave-induced panel movement, ensuring long-term durability and efficiency of the system.

4.1.2 *Battery and inverter*

A Battery Energy Storage System (BESS) adds essential flexibility to a PV system. Since solar power is variable and non-dispatchable, a BESS allows charging during off-peak hours and selling electricity to the grid during peak hours at higher rates. The levelized cost of capacity is reported as \$119 kW^{-1} $year^{-1}$ for a two-hour BESS and \$197 kWh^{-1} for a four-hour BESS.

For the analysis, a central inverter installed on land is assumed due to its lower cost compared to those installed on floats. All land-based components must meet appropriate IP ratings. A central inverter from SMA, specifically the SMA Sunny Central UP inverter, will be utilized in a 149 MWp FPV project located in Glenrowan West, Victoria.

With the PV panel and inverter models selected, their specifications will determine the minimum string size of the PV system. The minimum string size (N_S) is:

$$N_s = \frac{V_{MMPT}}{V_{module.min}} \tag{3}$$

where VMPPT is the Maximum Power Point Tracking voltage of the inverter, and $V_{module.min}$ is the expected minimum voltage of PV modules at high temperature, given as [44]:

$$V_{module.min} = V_{module.max} \times \left[1 + \left((T_{\max} + T_{add} - T_{stc}) \times \frac{Tk_{Vmax}}{100}\right)\right] \tag{4}$$

$V_{module.min}$ is the expected minimum module voltage at high ambient temperature.
$V_{module.max}$ is the rated maximum voltage of PV modules.
T_{max} is the maximum ambient temperature.
T_{add} is a temperature adjustment depending on the installation method.
T_{stc} is a typical ambient temperature.
Tk_{Vmax} is a PV module's temperature coefficient.

4.1.3 *Weather data*

Weather data were collected from the Australian Government's Bureau of Meteorology (BoM) [45]. The relevant data included ambient temperature, global irradiance, wind speed, and water temperature as shown in Table 3. The ambient temperature near the water is assumed to be 5 °C lower than the general ambient temperature due to the cooling effect of water. This assumption is supported by studies, such as the review by Trapani & Redón-Santafé [17], which demonstrates that large bodies of water, through evaporation and thermal regulation, can lower the surrounding air temperature and enhance the efficiency of FPV systems. Although this is not related to the wet-bulb temperature, it is a practical assumption used in calculating the performance improvements of FPV systems.

Table 3. Historical weather data of lake burrendong [45]

Months	Ambient temperature (°C)	Irradiance ($W \cdot m^{-2}$)	Wind velocity ($m \cdot s^{-1}$)	Water temperature (°C)
Jan	25	800.48	2.75	21.1
Feb	24.35	725.31	2.58	21.3
Mar	21.65	694.44	2.36	20.5
Apr	17.05	538.2	2.03	18.1
May	12.75	456.35	1.94	15.1
Jun	9.8	491.15	1.99	12.7
Jul	8.75	472.22	2.5	11.1
Aug	9.95	528.17	2.81	10.7
Sep	13.05	581.7	2.94	12.3
Oct	16.75	718.95	3.25	15
Nov	20.4	719.3	3.14	17.6
Dec	23.35	818.07	2.94	19.7

4.1.4 *Module temperature and efficiency*

A key characteristic of a PV module is its temperature coefficient, which directly affects its efficiency. The rated efficiency is measured at 25 °C, and any temperature variation impacts this efficiency. Using weather data from Australian Bureau of Meteorology (BoM) and the temperature coefficient of the Trina Solar 210 Vertex module, the panel temperature was calculated.

$$T_{GPV} = T_a + G_T \times e^{-3.473-0.0594\times V_w} \tag{5}$$

T_{GPV} is the panel temperature of a GPV panel.
T_a is the ambient temperature.
G_T is the global irradiance.
V_W is the wind velocity.

$$T_{FPV} = 1.8081 + 0.9282\,T_a + 0.021G_T - 1.2210V_w + 0.0246T_w \tag{6}$$

T_{FPV} is the panel temperature of an FPV panel.
T_a is the ambient temperature.
G_T is the global irradiance.
V_W is the wind velocity.
T_W is the water temperature.

Figure 7 shows the results of these calculations. Annually, FPV has an average temperature 5.51 °C lower than GPV in comparable conditions with the same irradiance and wind speed.

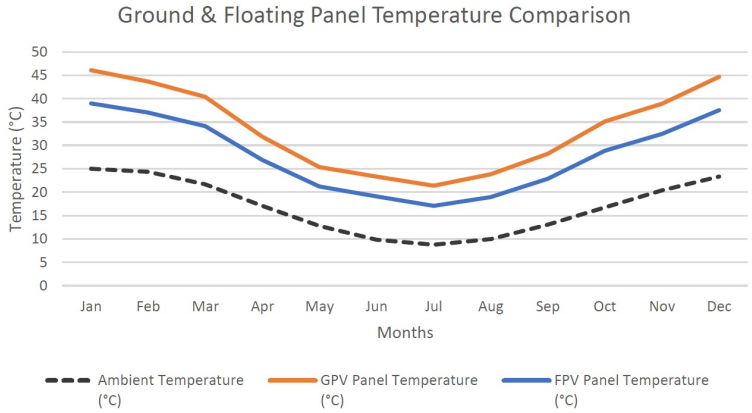

Figure 7. Ground and floating PV panel temperature comparison

This lower temperature improves efficiency, as shown in Figure 8, where FPV outperforms GPV by an average efficiency difference of 2.54%.

The efficiency of GPV and FPV are then calculated using the above panel temperatures.

$$E_{PV} = 100 - \left(T_{panel} - 25\right) \times 0.45 \tag{7}$$

E_{PV} is the efficiency of a PV module.
T_{panel} is the panel temperature calculated in Equations (5) and (6) for FPV and GPV.

Table 4 compares the relative efficiency and power output density of GPV and FPV. Although power density varies monthly, FPV consistently outperforms GPV.

Table 4. GPV and FPV's relative efficiency and their power output density

Months	GPV relative efficiency	FPV relative efficiency	GPV power output density (MW km^{-2})	FPV power output density (MW km^{-2})
Jan	90.51	93.71	78.79	81.57
Feb	91.61	94.59	72.26	74.61
Mar	93.08	95.9	70.29	72.42
Apr	96.92	99.14	56.73	58.03
May	99.83	101.7	49.55	50.47
Jun	100.75	102.65	53.81	54.83
Jul	101.63	103.57	52.19	53.19
Aug	100.53	102.71	57.74	59
Sep	98.56	100.97	62.35	63.87
Oct	95.44	98.27	74.62	76.83
Nov	93.74	96.65	73.32	75.6
Dec	91.15	94.35	81.09	83.94

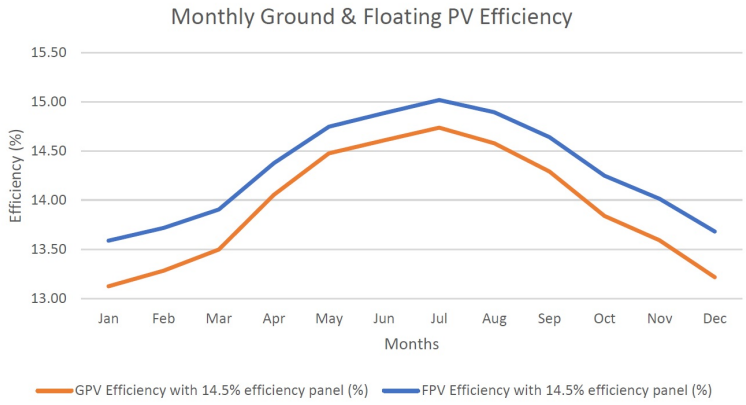

Figure 8. Monthly ground and floating PV panel efficiency given a panel with 14.5% rated efficiency

4.2 *Theoretical model*

4.2.1 *PV sizing*

To avoid overloading Burrendong Dam's substations, the PV system output installed was limited to 50% of the hydropower station's annual output, equating to 20 GWh year^{-1}. Using weather data from previous sections, a peak power of approximately 11,000 kWp is needed to generate 20 GWh year^{-1}.

Trina Solar's 210 Vertex 500 W modules will be used for their high efficiency [46], and SMA's central inverter was selected for its low cost [41]. PV system characteristics are shown in Table 5.

Table 5. PV system design summary

Parameters	Value (unit)
System peak power	11,000 kWp
Annual output	20 GWh year^{-1}
Number of modules	22,000
Module area	52,590 m^2
Number of inverters	4
Nominal PV power	11,006 kWp
Maximum PV power	10,871 kWDC
Nominal AC power	10,000 kWAC
Nominal power ratio	1.101

Figures 9 and 10 show the designed system on Lake Burrendong. Four sets of 2750 kWp islands, each 115 m wide, are depicted. With a total module area of 52,590 m^2, this 11,000 kWp FPV system would cover only 0.06% of the lake's 89 km^2 surface area.

Figure 9. Approximate real-life size of a 11,000 kWp PV system on lake Burrnedong

Figure 10. Zoomed out view of the same 11,000 kWp system

4.2.2 *Financial analysis*

Two key measurements of financial feasibility are used: LCOE and discounted payback rate. LCOE calculates the average cost of energy generated per kWh over the system's lifetime, making it essential for comparing different energy generation configurations. The discounted payback rate shows the number of years required to recoup the initial investment,

considering the discount rate. Lower LCOE and shorter payback periods are preferred as they indicate quicker returns and higher profits for investors.

$$LCOE = \frac{\frac{i(1+i)^n}{(1+i)^n-1} \times C_{npc}}{E_{served}} \tag{8}$$

where:
I: real discount rate
N: project lifetime
C_{npc}: net present cost
E_{served}: total electrical load served (kWh year^{-1})

$$Payback = -C_p \sum_{j=1}^{P} \frac{Q_j}{(1+i)^n} = 0 \tag{9}$$

where:
C_p: Capital cost
Q_j: Net cash flow for the year j
i: real discount rate

5. Simulation

To optimize the size and cost of PV systems, HOMER Pro software, developed by the US Department of Energy's NREL, is used. The software calculates and examines all possible configurations over a project's lifespan based on various inputs, such as daily solar irradiance and dispatch methods for selling power to the grid, as listed in Table 5.

5.1 *Grid rate*

The grid sellback rate, the price at which the grid buys electricity from the system, will be the primary source of cash inflow, aside from the small residual value of system components at the project's end. This rate is crucial. The Australian Energy Market Operator (AEMO) publishes historic spot price data for NSW at 5-min intervals. Figure 10 illustrates this data, with the teal line showing real-time demand and the purple line showing the current spot price. Spot prices fluctuate with demand, and the recent energy crisis in Australia has exacerbated these fluctuations, causing wholesale energy prices to rise by 141% in 2022 compared to the previous year. Although prices are expected to rise further, the simulation used January to December 2021 data due to the unpredictability of the recent price spike.

Figure 11 shows that the grid sellback rate is highly variable and depends on real-time demand. These fluctuations can lead to higher revenue during peak periods but also make revenue forecasting challenging. Therefore, 2021 data was used for simulation to provide a more stable basis for financial projections despite recent price spikes.

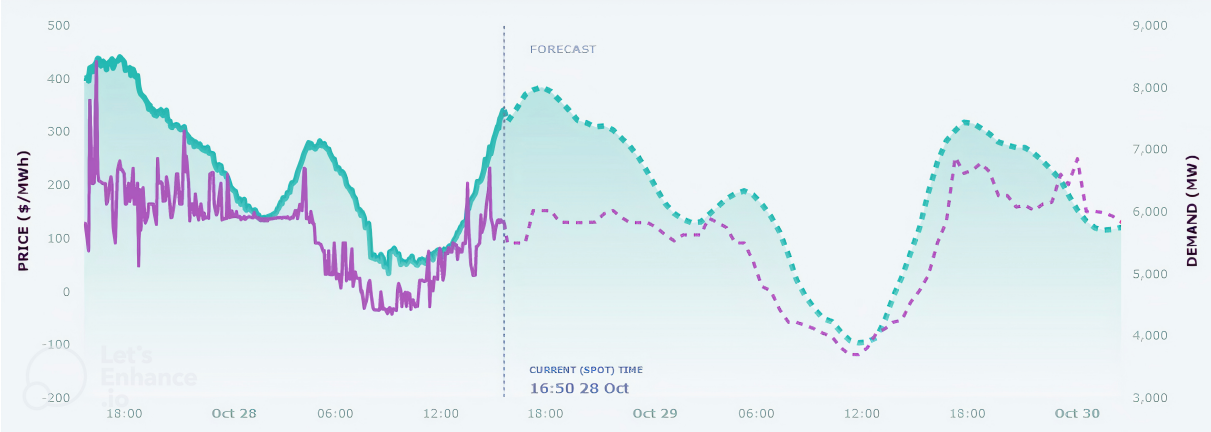

Figure 11. Example of spot prices in NSW, compiled from publicly available data on the AEMO NEM Data Dashboard [47]. This figure is used for illustrative purposes based on aggregated information available for public use

5.2 *Weather data*

As shown in Equation (6), the key weather data for the project are solar irradiance, ambient temperature, and wind velocity. This data, obtained from the Bureau of Meteorology, is considered accurate for the project. Figures 12–14 show the monthly average solar irradiance, ambient temperature, and wind speed at Lake Burrendong, used for the simulation.

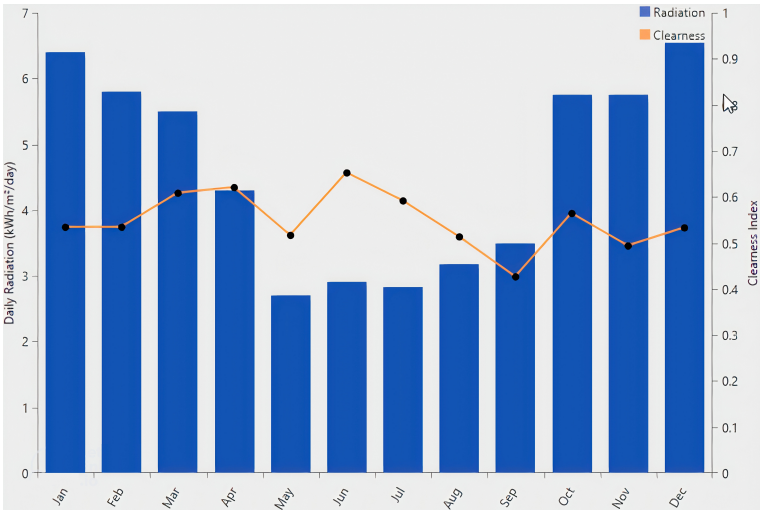

Figure 12. Monthly solar irradiance as inputted for simulation

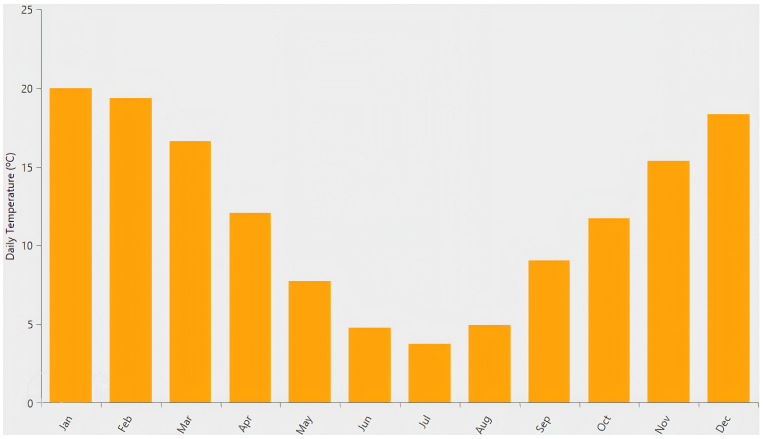

Figure 13. Monthly average temperature data for simulation

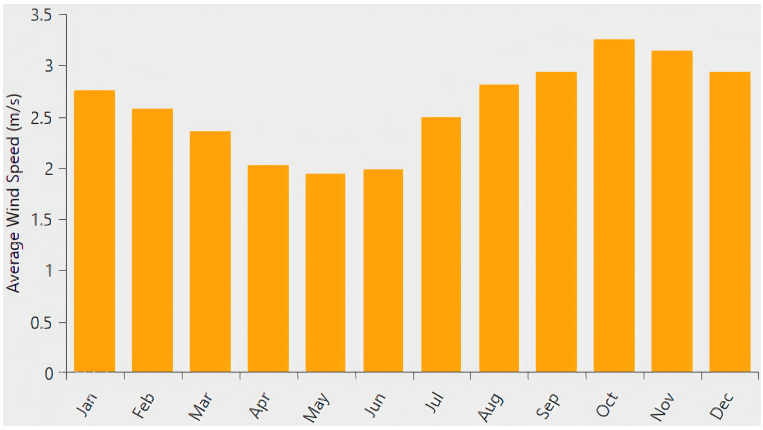

Figure 14. Monthly average wind speed for simulation

5.3 *System configuration*

Figure 15 illustrates the simulated system configuration. Energy produced by the FPV system will either be stored in the BESS or sold to the grid at the spot price.

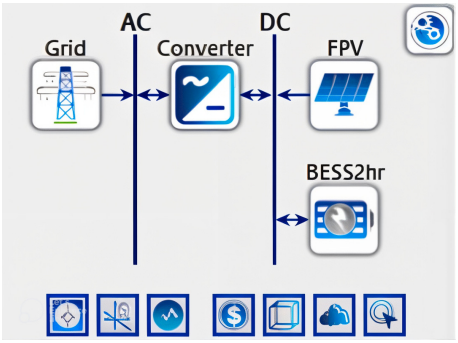

Figure 15. High-level diagram of a FPV system

Figure 16 illustrates the grid rate schedule, specifying the on-peak and off-peak times throughout the year, which controls when energy is stored or sold to the grid based on the grid sellback rate. The blue parts indicate times during the day when solar radiation is not available, and the plant is not generating electricity. The yellow parts represent off-peak times, and the red parts indicate peak times.

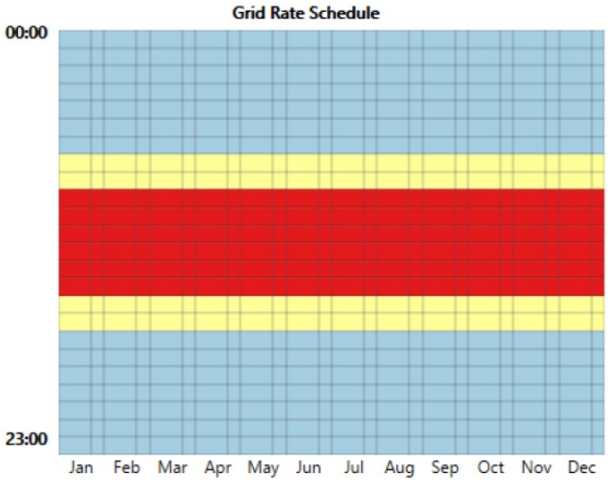

Figure 16. Monthly weekday grid rate schedule

6. Results and discussions

The results of our simulation highlight the dynamic relationship between FPV output, BESS charge-discharge cycles, and grid sellback rates (see Figure 17), demonstrating the potential for optimized energy management in hybrid systems. By utilizing existing transmission capacity and coupling FPV with HPPs, we achieve not only improved energy efficiency but also the preservation of water resources through reduced evaporation. These outcomes underscore the significance of our findings in the context of Australia's environmental challenges and renewable energy targets. The payback period for the proposed system, while longer than smaller configurations, offers significant long-term savings and environmental benefits, positioning FPV-HPP systems as viable options for sustainable energy development in the region.

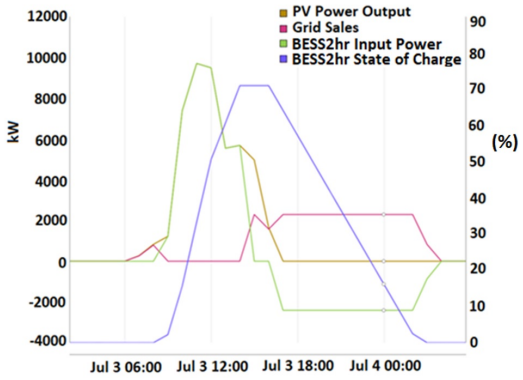

Figure 17. Line chart illustrating grid sales strategy

To determine the best system configuration for pairing with Burrendong hydropower station, various PV and BESS sizes were simulated within the maximum annual output limit. Figure 18 shows the impact of BESS size on capital

investment and payback rate, with the red line indicating optimal BESS sizes for each PV size. These optimal sizes are summarized in Table 6. LCOE is divided into two categories: before and after grid sales. Since total revenue exceeds investment costs over the project's lifetime, the LCOE after grid sales is negative, indicating average profit per MWh.

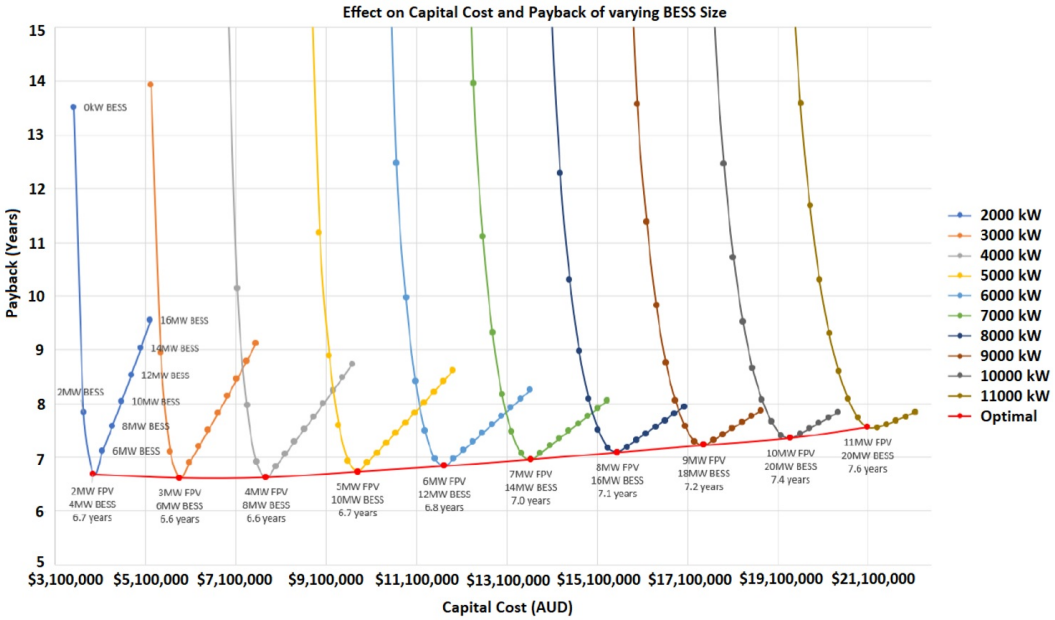

Figure 18. Effect on Capital Cost and Payback of varying BESS size

The results indicate that a system with 4 MW PV and 4 MW/8 MWh BESS has the lowest payback period (6.6 years) and LCOE. Although this system recovers the initial investment quickest, a larger system is recommended to fully utilize Burrendong hydropower station's available transmission capacity.

A system with 11 MW PV and 22 MW/44 MWh BESS would maximize this capacity, generating 20 GWh year^{-1}, about 2.75 times more energy than the 4 MW system. The payback period is 14% longer, taking 7.6 years, just one year more than the smaller system.

Table 6. Summary of simulation results

FPV size	Optimal BESS size	Discounted payback rate	LCOE before grid sale	LCOE after grid sale
2 MW	4 MW / 8 MWh	6.7 years	98.64 $/MWh	−166 $/MWh
3 MW	6 MW / 12 MWh	6.6 years	98.46 $/MWh	−167 $/MWh
4 MW	8 MW / 16 MWh	6.6 years	96.82 $/MWh	−167 $/MWh
5 MW	10 MW / 20 MWh	6.7 years	97.90 $/MWh	−166 $/MWh
6 MW	12 MW / 24 MWh	6.8 years	97.42 $/MWh	−165 $/MWh
7 MW	14 MW / 28 MWh	7.0 years	97.06 $/MWh	−164 $/MWh
8 MW	16 MW / 32 MWh	7.1 years	96.81 $/MWh	−163 $/MWh
9 MW	18 MW / 36 MWh	7.2 years	96.61 $/MWh	−162 $/MWh
10 MW	20 MW / 40 MWh	7.4 years	96.44 $/MWh	−161 $/MWh
11 MW	22 MW / 44 MWh	7.6 years	96.32 $/MWh	−158 $/MWh

A similar analysis, shown in Figure 18, was conducted with GPV systems, and their results were compared with FPV systems in Table 7. At the lowest-cost size of 4 MW, GPV has a 14% faster payback rate and 9% lower LCOE than FPV. At the recommended size of 11 MW to fully utilize the underused transmission capacity, GPV has a 16% faster payback rate and 9.1% lower LCOE than FPV.

Table 7. Summary of FPV & GPV comparison

	PV size	BESS size	Discounted payback rate	LCOE before grid sale	LCOE after grid sale
Optimal FPV size	4 MW	8 MW / 16 MWh	6.6 years	96.82 $/MWh	−167 $/MWh
Optimal GPV size	4 MW	8 MW / 16 MWh	5.7 years	88.15 $/MWh	−177 $/MWh
Recommended FPV size	11 MW	22 MW / 44 MWh	7.6 years	96.32 $/MWh	−158 $/MWh
Recommended GPV size	11 MW	22 MW / 44 MWh	6.4 years	87.65 $/MWh	−170 $/MWh

To compare the power output of a hybrid FPV and HPP station, the Burrendong Dam with a recommended 11 MW FPV and 22 MW/44 MWh BESS was simulated. Figure 19 shows the annual power output of Burrendong HPP without FPV, and Figure 20 shows the annual power output of Burrendong HPP with 11 MW FPV. The calculations indicate that the annual output of the FPV does not exceed 50% of Burrendong HPP's annual power output to avoid overloading the existing transmission infrastructure.

By comparing the optimal payback period and LCOE for the recommended FPV size without BESS, it could be observed that the payback period and LCOE for an 11 MW PV system have improved by approximately 6.5%. This indicates a significant reduction in the annual cost of energy for FPV systems when storage is not included, highlighting the impact of storage costs.

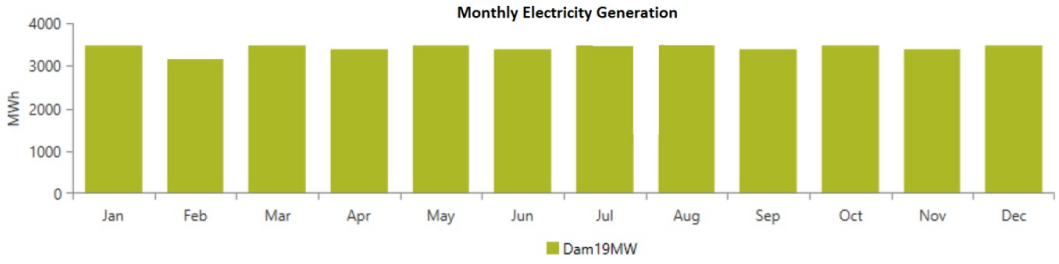

Figure 19. Power output of a HPP without FPV

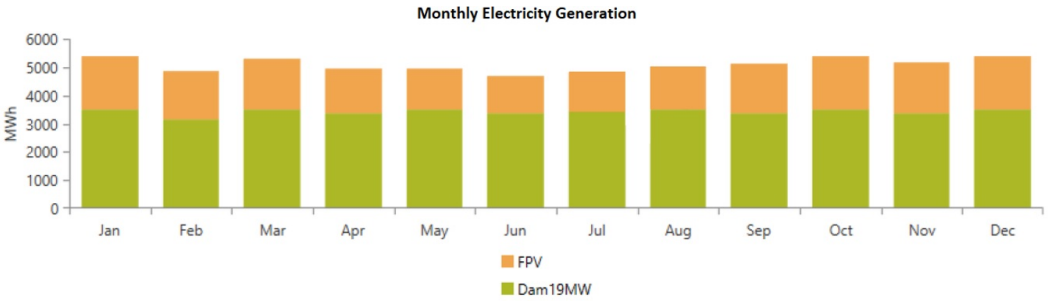

Figure 20. Power output of a HPP & FPV hybrid power station

7. Conclusions

The study demonstrates that FPV systems at Burrendong Dam exhibit a 2.54% improvement in efficiency over GPV systems, attributed to the water's cooling effect, which reduces panel temperature by an average of 5.51 °C. Integrating FPV with hydropower infrastructure at the dam has the potential to enhance annual energy output by up to 10%, yielding approximately 20 GWh/year while also significantly decreasing water evaporation by up to 49%. This dual benefit of energy efficiency and water conservation highlights FPV's relevance for drought-prone regions in Australia. However, the

FPV system has a 9% higher LCOE compared to GPV due to the additional costs of floating infrastructure. Despite the higher initial investment, excluding battery storage improves the payback period for the FPV system by 6.5%, enhancing its economic viability under specific conditions.

Future advancements in FPV systems should focus on improving efficiency, reducing costs, and addressing environmental impacts. Technological innovations, such as lightweight and corrosion-resistant materials, can enhance modularity and long-term performance. While FPV systems offer benefits like reduced land use, improved cooling efficiency, and water evaporation control, challenges such as higher upfront costs and potential aquatic ecosystem impacts require strategic solutions. Strengthening economic viability through government subsidies, public-private partnerships, and supportive policies, including streamlined permitting and tax incentives, can accelerate adoption. Furthermore, studies on ecological interactions, shading effects, and long-term system performance are essential to ensure sustainable deployment. Stakeholder engagement, along with robust regulatory frameworks, will play a pivotal role in driving the global adoption of FPV systems, advancing renewable energy solutions for both energy and water resource management.

Conflict of interests

There is no conflict of interest declared by the authors.

References

[1] International Energy Agency (IEA), "Electricity 2024: Analysis and forecast to 2026." Accessed: Mar. 13, 2023. [Online]. Available: https://www.iea.org/reports/electricity-2024.

[2] International Renewable Energy Agency (IRENA), "Renewable Power Generation Costs in 2022." Accessed: Mar. 13, 2023. [Online]. Available: https://www.irena.org/Publications/2023/Aug/Renewable-Power-Generation-Costs-in-2022.

[3] Department of Climate Change, Energy, the Environment and Water, "Australian Energy Statistics, Table O: Electricity generation by fuel type 2022-23 and 2023." Accessed: Mar. 13, 2023. [Online]. Available: https://www.energy.gov.au/publications/australian-energy-statistics-table-o-electricity-generation-fuel-type-2022-23-and-2023.

[4] International Energy Agency (IEA), "Snapshot of Global PV Markets 2024." Accessed: Mar. 13, 2023. [Online]. Available: https://iea-pvps.org/wp-content/uploads/2024/04/Snapshot-of-Global-PV-Markets_20241.pdf.

[5] P. Simshauser, "Renewable Energy Zones in Australia's National Electricity Market," *Energy Econ.*, vol. 101, p. 105446, 2021. https://doi.org/10.1016/j.eneco.2021.105446.

[6] F. Biermann, N. Kanie, and R. E. Kim, "Global governance by goal-setting: The novel approach of the UN Sustainable Development Goals," *Curr. Opin. Environ. Sustain.*, vol. 26–27, pp. 26–31, 2017. https://doi.org/10.1016/j.cosust.2017.01.010.

[7] J. Zalk and P. Behrens, "The spatial extent of renewable and non-renewable power generation: A review and meta-analysis of power densities and their application in the U.S.," *Energy Policy*, vol. 123, pp. 83–91, 2018. https://doi.org/10.1016/j.enpol.2018.08.023.

[8] S. Schlömer, T. Bruckner, L. Fulton, E. Hertwich, A. McKinnon, D. Perczyk, et al., *Annex III: Technology-Specific Cost and Performance Parameters*. Cambridge, UK: Cambridge University Press, 2014.

[9] D. Murphy, M. Raugei, M. Carbajales-Dale, and B. Rubio Estrada, "Energy Return on Investment of Major Energy Carriers: Review and Harmonization," *Sustainability*, vol. 14, no. 12, p. 7098, 2022. https://doi.org/10.3390/su14127098.

[10] C. L. W. Kamuyu, J. R. Lim, C. S. Won, and H. K. Ahn, "Prediction Model of Photovoltaic Module Temperature for Power Performance of Floating PVs," *Energies*, vol. 11, no. 2, p. 447, 2018. https://doi.org/10.3390/en11020447.

[11] A. P. Sukarso and K. N. Kim, "Cooling Effect on the Floating Solar PV: Performance and Economic Analysis on the Case of West Java Province in Indonesia," *Energies*, vol. 13, no. 9, p. 2126, 2020. https://doi.org/10.3390/en13092126.

[12] R. S. Spencer, J. Macknick, A. Aznar, A. Warren, and M. O. Reese, "Floating photovoltaic systems: Assessing the technical potential of photovoltaic systems on man-made water bodies in the continental United States," *Environ. Sci. Technol.*, vol. 53, no. 3, pp. 1680–1689, 2019. https://doi.org/10.1021/acs.est.8b04735.

[13] L. Liu, Q. Wang, H. Lin, H. Li, Q. Sun, "Power generation efficiency and prospects of floating photovoltaic systems," *Energy Proc.*, vol. 105, pp. 1136–1142, 2017. https://doi.org/10.1016/j.egypro.2017.03.451.

[14] M. Salman, "Design of an on-grid floating solar photovoltaic system: A case of Vaigai Dam in Tamil Nadu," in *Control Applications in Modern Power Systems*, S. Kumar, M. Tripathy, and P. Jena, Eds. Singapore: Springer, 2024, vol. 1128. https://doi.org/10.1007/978-981-99-9054-2_4.

[15] N. Yadav, M. Gopi, and K. Sudhakar, "Energy assessment of floating photovoltaic system," in *Proc. 2016 Int. Conf. Electr. Power Energy Syst. (ICEPES)*, Bhopal, India, Dec. 14–16, 2016.

[16] V. Durkovic and Z. Durisic, "Analysis of the potential for use of floating PV power plant on the Skadar Lake for electricity supply of aluminium plant in Montenegro," *Energies*, vol. 10, p. 1505, 2017. https://doi.org/10.3390/en10101505.

[17] K. Trapani and M. Redón Santafé, "A review of floating photovoltaic installations," *Progress Photovoltaics Res. Appl.*, vol. 23, pp. 524–532, 2015. https://doi.org/10.1002/pip.2470.

[18] Z. A. A. Majid, M. H. Ruslan, K. Sopian, M. Y. Othman, M. S. M. Azmi, "Study on performance of 80 watt floating photovoltaic panel," *J. Mech. Eng. Sci.*, vol. 7, pp. 1150–1156, 2014. https://doi.org/10.15282/jmes.7.2014.14.0112.

[19] Y. G. Lee, H. J. Joo, and S. J. Yoon, "Design and installation of floating type photovoltaic energy generation system using FRP members," *Sol. Energy*, vol. 108, pp. 13–27, 2014. https://doi.org/10.1016/j.solener.2014.05.035.

[20] M. S. M. Azmi, M. Y. H. Othman, M. H. H. Ruslan, K. Sopian, Z. A. A. Majid, "Study on electrical power output of floating photovoltaic and conventional photovoltaic," *AIP Conf. Proc.*, vol. 1554, no. 1, pp. 95–101, 2013. https://doi.org/10.1063/1.4823927.

[21] Y. K. Choi, "A study on power generation analysis of floating PV system considering environmental impact," *Int. J. Softw. Eng. Its Appl.*, vol. 8, no. 1, pp. 75–84, 2014. https://doi.org/10.14257/ijseia.2014.8.1.07.

[22] N. M. Kumar, S. Islam, A. K. Podder, A. Selim, M. Bajaj, S. Kamel, "Lifecycle-based feasibility indicators for floating solar photovoltaic plants along with implementable energy enhancement strategies and framework-driven assessment approaches leading to advancements in the simulation tool," *Front. Energy Res.*, vol. 11, p. 1075384, 2023. https://doi.org/10.3389/fenrg.2023.1075384.

[23] C. J. Ramanan, K. H. Lim, J. C. Kurnia, S. Roy, B. J. Bora, B. J. Medhi, "Towards sustainable power generation: Recent advancements in floating photovoltaic technologies," *Renew. Sustain. Energy Rev.*, vol. 194, p. 114322, 2024. https://doi.org/10.1016/j.rser.2024.114322.

[24] M. A. Rahaman, T. L. Chambers, A. Fekih, G. Wiecheteck, G. Carranza, G. R. C. Possetti, "Floating photovoltaic module temperature estimation: Modeling and comparison," *Renew. Energy*, vol. 208, pp. 162–180, 2023. https://doi.org/10.1016/j.renene.2023.03.076.

[25] M. Rosa-Clot and G. M. Tina, *Submerged and Floating Photovoltaic Systems*. Amsterdam, The Netherlands: Elsevier, 2018, pp. 13–32.

[26] M. Fereshtehpoura, R. J. Sabbaghian, A. Farrokhi, E. B. Jovein, and E. E. Sarindizaje, "Evaluation of factors governing the use of floating solar system: A study on Iran's important water infrastructures," *Renew. Energy*, vol. 171, pp. 1171–1187, 2021. https://doi.org/10.1016/j.renene.2021.03.055.

[27] R. Snead, "Floating a New Solution for Solar Deployment," Environmental and Energy Study Institute, Mar. 30, 2021. Accessed: Apr, 1, 2022. [Online]. Available: https://www.eesi.org/articles/view/floating-a-new-solution-for-solar-deployment.

[28] F. B. Scavo, G. M. Tina, A. Gagliano, and S. Nižetić, "An assessment study of evaporation rate models on a water basin with floating photovoltaic plants," *Energy Res.*, vol. 45, no. 1, pp. 167–188, 2021. https://doi.org/10.1002/er.5600.

[29] J. Haas, J. Khalighi, P. J. Chen, A. De La Fuente, and W. Nowak, "Save the Lake! Floating Solar Photovoltaic to Avoid Algae Blooms?" in *American Geophysical Union*. American Geophysical Union: Washington, DC, USA, 2018.

[30] F. J. F. Orozco and C. Breyer, "Combining Floating Solar Photovoltaic Power Plants and Hydropower Reservoirs: A Virtual Battery of Great Global Potential," *Energy Proced.*, vol. 155, pp. 403–411, 2018.

[31] K. Chen, Y. Jin, Y. Feng, W. Song, Y. Li, Y. Zhou, et al., "Floating solar power as an alternative to hydropower expansion along China's Yellow River," *Resources, Conserv. Recycl.*, vol. 207, p. 107689, 2024. https://doi.org/10.1016/j.resconrec.2024.107689.

[32] "Burrendong Dam falls below Flood Mitigation Zone for first time in 15 months," Water NSW. Accessed: Mar. 13, 2023. [Online]. Available: https://www.waternsw.com.au/community-news/media-releases/2023/burrendong-dam-falls-below-flood-mitigation-zone-for-first-time-in-15-months.

[33] V. Durkovic and Z. Durisic, "Analysis of the Potential for Use of Floating PV Power Plant on the Skadar Lake for Electricity Supply of Aluminium Plant in Montenegro," *Energies*, vol. 10, p. 1505, 2017. https://doi.org/10.3390/en10101505.

[34] D. Mathijssen, B. Hofs, E. Spierenburg-Sack, R. van Asperen, B. van der Wal, J. Vreeburg, et al., "Potential impact of floating solar panels on water quality in reservoirs; pathogens and leaching," *Water Pract. Technol.*, vol. 15, no. 3, pp. 807–811, 2020. https://doi.org/10.2166/wpt.2020.065.

[35] S. Robinson and G. Meindl, "Potential for leaching of heavy metals and metalloids from crystalline silicon photovoltaic systems," *J. Nat. Resour. Dev.*, vol. 9, pp. 19–24, 2019.

[36] A. Sen, A. S. MohanKar, A. Khamaj, and S. Karmakar, "Emerging OSH Issues in Installation and Maintenance of Floating Solar Photovoltaic Projects and Their Link with Sustainable Development Goals," *Risk Manag. Healthc. Policy*, vol. 14, pp. 1939–1957, 2021. https://doi.org/10.2147/RMHP.S302768.

[37] C. Lin, "Singapore unveils one of the world's biggest floating solar panel farms," *Reuters*, Jul. 15, 2021. Accessed: May, 5, 2022. [Online]. Available: https://www.reuters.com/business/energy/singapore-unveils-one-worlds-biggest-floating-solar-panel-farms-2021-07-14/.

[38] Solar Energy Research Institute of Singapore (SERIS), World Bank, International Finance Corporation (IFC), *Where Sun Meets Water*. Washington, DC, USA: World Bank Group, 2019.

[39] S. Semeskandeh, M. Hojjat, and M. Hosseini Abardeh, "Techno-economic-environmental comparison of floating photovoltaic plant with conventional solar photovoltaic plant in northern Iran," *Clean Energy*, vol. 6, no. 2, pp. 353–361, 2022. https://doi.org/10.1093/ce/zkac019.

[40] "Burrendong Dam falls below Flood Mitigation Zone for first time in 15 months," Water NSW. Accessed: Mar. 13, 2023. [Online]. Available: https://www.waternsw.com.au/community-news/media-releases/2023/burrendong-dam-falls-below-flood-mitigation-zone-for-first-time-in-15-months.

[41] V. Ramasamy and R. Margolis, *Floating Photovoltaic System Cost Benchmark: Q1 2021 Installations on Artificial Water Bodies*. Golden, CO, USA: National Renewable Energy Laboratory, 2021. https://doi.org/10.2172/1804566.

[42] S. Mahmood, S. Deilami, and S. Taghizadeh, "Floating solar PV and hydropower in Australia: feasibility, future investigations and challenges," in *Proc. 2021 31st Australas. Univ. Power Eng. Conf. (AUPEC)*, Perth, Australia, Sept. 26–30, 2021.

[43] H. Liu, A. Kumar, and T. Reindl, "The Dawn of Floating Solar—Technology, Benefits, and Challenges," in *WCFS2019*, C. Wang, S. Lim, and Z. Tay, Eds., Singapore: Springer: Lecture Notes in Civil Engineering, 2020, vol. 41. https://doi.org/10.1007/978-981-13-8743-2_21.

[44] R. A. Messenger and A. Abtahi, *Photovoltaic Systems Engineering*, 4th ed. Boca Raton, FL, USA: CRC Press, 2017.

[45] Bureau of Meteorology, "Climate statistics for Australian locations," Bureau of Meteorology. Accessed: Mar. 13, 2023. [Online]. Available: http://www.bom.gov.au/climate/averages/tables/cw_065034_All.shtml.

[46] Trina Solar, "Vertex S 210 mm ultra-high power modules," Trina Solar [Internet]. Accessed: Oct. 22, 2024. [Online]. Available: https://pages.trinasolar.com/DE18M.html.

[47] AEMO, "Data Dashboard," Oct. 28, 2022. Accessed: Mar. 13, 2023. [Online]. Available: https://aemo.com.au/en/energy-systems/electricity/national-electricity-market-nem/data-nem/data-dashboard-nem.